Prediction of the Effect of Polymer Membrane Composition in a Dry Air Humidification Process via Neural Network Modeling

M. Fakhroleslam[a, 1], A. Samimi[a], S. A. Mousavi [a,*], R. Rezaei[b]

[a] *Chemical and Petroleum Engineering Department, Sharif University of Technology, Tehran, Iran*
[b] *Chemical Engineering Department, Razi University, Kermanshah, Iran*

Abstract
Utilization of membrane humidifiers is one of the methods commonly used to humidify reactant gases in polymer electrolyte membrane fuel cells. In this study, polymeric porous membranes with different compositions were prepared to be used in a membrane humidifier module and were employed in a humidification test. Three different neural network models were developed to investigate several parameters, such as casting solution composition and operating conditions, which have an impact on relative humidity of the exhausted air after humidification process. The three mentioned models included Feed-Forward Back-Propagation (FBP), Radial Basis Function (RBF), and Feed-Forward Genetic Algorithm (FFGA). The models were verified by experimental data. The results showed that the feed-forward models, especially FFGA, were suitable for this type of membrane humidifiers.

Keywords: *Membrane Humidifier, Membrane Contactor, Dry Air, Neural Network Modeling, Genetic Algorithm*

*Corresponding author: musavi@sharif.edu

1. Introduction

Nowadays, the application of membrane processes in laboratories and industries has received much attention and many studies have been conducted on this subject. Among these processes, membrane contactors are of great importance [1]. The membrane contactors were first applied for dissolving oxygen in blood in the 1970s [2]. Later, the membrane contactors were applied in many different fields such as natural gas purification, humidity control, and organic gases elimination [3]. In a membrane contactor, membrane acts as a media between gas and liquid phases and can be used to solve many problems in the fields of food and pharmaceutical industries, foaming, entraining and channeling industries [4].

As one of the applications of the membrane contactors, they are used in humidifiers that are employed in Polymer Electrolyte Membrane Fuel Cells (PEMFC). In these fuel cells the electrolyte is composed of a polymeric membrane with the ability to conduct H^+; to have a good performance, this membrane must be wetted. Perfluorosulfonate membranes are usually utilized in the PEMFCs and their proton conductivity is reduced by decreasing the water content of membrane [5]. Membrane humidification is affected by water transfer phenomena in the membrane and is associated with the condition of reactant gases and operating parameters of the fuel cell. Therefore, the water content in the electrolyte can be controlled via determining the condition of inlet gases. There are different ways to humidify reactant gases; however, the membrane humidifiers are preferred because they occupy a small space, consume low amounts of energy, and have a good performance.

In a membrane humidifier, dry gas passes one side of the membrane while liquid water or water vapor passes the other side. Because of the chemical potential gradient, water passes the membrane from wet to dry stream, and reactant gas will be humidified. Chen *et al.* [6], investigated the behavior of a membrane humidifier in dynamic and static states and developed a thermodynamic model in their study. The results obtained in the static state showed that the water vapor transfer rate increased with an increase in water channel temperature, gas channel temperature, and gas flow rate. Since water channel pressure had an insignificant effect, the researchers ignored it in the modeling. [7] studied a membrane humidifier, utilizing Nafion membranes. They introduced a one-dimensional analytical model for measuring humidification capacity of the Nafion membrane humidifiers. Their model predicted the humidity content as a function of length and height of gas channel that was consistent with the experimental data. In another study, Choe *et al*. developed a mathematical model for Nafion shell and tube membrane humidifiers [8]. The model was designed for gas to gas humidifiers and included geometrical and operational parameters based on thermodynamic principles. Merida *et al*. conducted experiments on a commercial humidifier with a porous membrane and analyzed experimental data under a model for heat and mass transfer [9].

Artificial neural networks are applied for several membrane processes [10-16]. Shokrian *et al*. [15] utilized a multilayer perceptron (MLP) that was trained by Levenberg–Marquardt back propagation method to predict the separation factor of C_3H_8 for different inputs of training experimental data. Shahsavand and Chenar [13] compared the performance of two different Radial Basis Function (RBF) and MLP networks for prediction of hollow fiber permeances and the corresponding separation factors. Chakraborty *et al*. [10] studied the application of neural networks for prediction of solute concentration in feed during extraction operation and its ultimate extraction percentage. In recent studies about the membrane humidifiers, there has been no focus on membrane synthesis and its parameters. Previous studies have investigated commercial membranes through utilizing thermodynamic modeling. This study focuses on the preparation of porous membranes and it aims to introduce a suitable neural network model for investigating the effects of preparation factors and operational conditions on humidification process. The numerical model was also verified using the experimental data reported in the previous study [17].

2. Experimental setup
2-1. Membrane preparation method
The membranes were prepared via wet phase inversion process. For this purpose, casting solutions were prepared with different compositions of polymer in N-methyl-2-pyrrolidone (NMP) and Dimethylformamide (DMF) solvents. For synthesis of the nano-composite membranes, titanium dioxide nano-particles were used. After mixing the solutions for 24 h with a magnet stirrer, the casting solution was dispersed on a glass support using a casting machine at room temperature. Then, the polymer films were floated in a coagulation bath containing deionized water and remained there until the inversion process phase was completed.

Different structures of membrane cavities from finger type to sponge like structures were observed. Also, adding TiO_2 nanoparticles enhanced the humidification due to increase in the membrane hydrophilicity.

2-2. Humidification test
Fig. 1 shows the humidification setup for measuring relative humidity (RH) of the outlet gas and the humidification membrane module, respectively. Membrane module was assembled using a membrane with two different flow fields for the dry air gas and the liquid water. Pressure, temperature, and flow rate of gas and water were controlled in the system and gas RH was measured by a humidity indicator (Lutron HT-315). Because the membranes were porous, the pressure was constant and equal on both sides of the membrane and water transfer occurred due to the difference in chemical potentials. Hence, the flow rate of water was very low and the main concerns on waterside were presence of water at a specific pressure and temperature that were indicated in each experiment. The temperature was fixed in

the system by a water bath equipped with a temperature controller and a mechanical mixer. The gas flow field was a serpentine channel with a specific length, 5 mm width, and 6 mm of surface contact with the membrane. The effective surface of the membrane in the module was 5676 mm^2. The water flow field was a simple container with a reticular plate to hold the membrane. By using this apparatus, it was possible to investigate the effects of the operating conditions and the membrane synthesis parameters on humidification. Composition of casting solution was an important factor affecting the shape, position, and orientation of the formed cavities, which have certain effects on humidification performance. The RH decreased by increasing the gas flow rate, the flow channel pressure, and the module temperature. A total of 69 membranes were prepared and the experimental data were recorded as Table 1. Also, mechanical characteristics of the fabricated membranes are reported in Table 2. For more details on membrane characterization, the reader is referred to [17].

Table 1

Experimental data of the humidification set-up.

No.	Polymer	Solvent	Polymer weight %	Thickness (μm)	Pressure (bar)	Flow rate (L/h)	Temperature (°C)	RH (%)	No.	Polymer	Solvent	Polymer weight %	Thickness (μm)	Pressure (bar)	Flow rate (L/h)	Temperature (°C)	RH (%)
1	PES	DMF	16	50	1	60	29.94	68.30	36	PSU	DMF	7	50	1	180	32.65	67.55
2	PES	DMF	16	50	1	120	30.22	67.66	37	PSU	DMF	16	50	1	60	34.00	85.65
3	PES	DMF	16	50	1	180	29.94	62.70	38	PSU	DMF	16	50	1	120	32.17	77.55
4	PES	DMF	16	50	2	60	30.02	60.25	39	PSU	DMF	16	50	1	180	32.65	70.72
5	PES	DMF	16	50	3	60	30.27	43.05	40	PSU	DMF	16	50	2	60	33.70	72.52
6	PES	DMF	10	50	1	60	30.53	74.49	41	PSU	DMF	16	50	3	60	33.50	68.52
7	PES	DMF	10	50	1	120	30.57	73.62	42	PSU	DMF	16	60	1	60	32.01	70.66
8	PES	DMF	10	50	1	180	30.44	67.60	43	PSU	DMF	16	60	1	120	31.59	65.83
9	PES	DMF	10	50	1	300	29.57	66.15	44	PSU	DMF	16	60	1	180	31.60	62.75
10	PES	DMF	10	50	2	60	29.80	71.68	45	PSU	DMF	16	60	1	300	30.20	62.70
11	PES	DMF	10	50	3	60	29.96	70.50	46	PSU	DMF	16	60	2	60	31.40	60.96
12	PES	DMF	7	50	1	60	31.51	70.04	47	PSU	DMF	16	200	1	60	31.72	56.50
13	PES	DMF	7	50	1	120	31.24	64.96	48	PSU	DMF	16	200	1	120	31.00	59.41
14	PES	DMF	7	50	1	180	32.32	63.09	49	PSU	DMF	16	200	1	180	31.12	51.53
15	PES	DMF	7	50	2	60	32.12	57.28	50	PSU	DMF	16	200	1	300	30.62	51.96
16	PES	DMF	7	50	3	60	31.40	64.00	51	PES	DMF	16	50	1	60	32.25	75.30
17	PES	DMF	10	100	1	60	30.97	53.50	52	PES	DMF	16	50	1	120	32.22	73.60
18	PES	DMF	10	100	1	120	30.95	47.10	53	PES	DMF	16	50	1	180	32.32	65.80
19	PES	DMF	10	100	1	180	30.97	46.30	54	PSU	NMP	16	50	1	60	32.00	79.87
20	PES	DMF	10	100	1	300	30.90	45.98	55	PES	NMP	16	50	1	60	32.00	76.00

21	PES	DMF	10	100	2	60	31.08	39.80	**56**	PES	NMP	16	50	1	60	32.00	81.00
22	PES	DMF	16	100	1	60	30.59	46.53	**57**	PES	NMP	16	50	1	60	32.50	76.31
23	PES	DMF	16	100	1	120	30.62	45.45	**58**	PES	NMP	16	50	1	120	32.60	75.42
24	PES	DMF	16	100	1	180	30.51	44.36	**59**	PES	NMP	16	50	1	180	31.77	67.70
25	PES	DMF	16	100	2	60	30.64	39.44	**60**	PES	NMP	16	50	2	60	31.80	75.51
26	PES	DMF	16	100	3	60	30.54	33.46	**61**	PES	NMP	16	50	2	120	32.00	63.85
27	PSU	DMF	16	50	1	60	31.00	75.00	**62**	PES	NMP	16	50	2	180	32.00	61.69
28	PSU	DMF	10	50	1	60	32.86	76.60	**63**	PES	NMP	16	50	3	60	31.87	72.50
29	PSU	DMF	10	50	1	120	32.87	70.67	**64**	PES	NMP	16	50	1	60	31.65	71.28
30	PSU	DMF	10	50	1	180	32.75	60.57	**65**	PES	NMP	16	50	1	120	30.86	70.39
31	PSU	DMF	10	50	1	300	31.08	64.11	**66**	PES	NMP	16	50	1	180	30.09	64.51
32	PSU	DMF	10	50	2	60	32.97	69.92	**67**	PES	NMP	16	50	1	240	30.00	63.54
33	PSU	DMF	10	50	3	60	33.12	63.43	**68**	PES	NMP	16	50	2	60	29.97	71.15
34	PSU	DMF	7	50	1	60	32.50	73.51	**69**	PES	NMP	16	50	3	60	29.90	70.78
35	PSU	DMF	7	50	1	120	32.22	70.68	**-**								

Table 2
Mechanical characteristics of the fabricated polymer membranes.

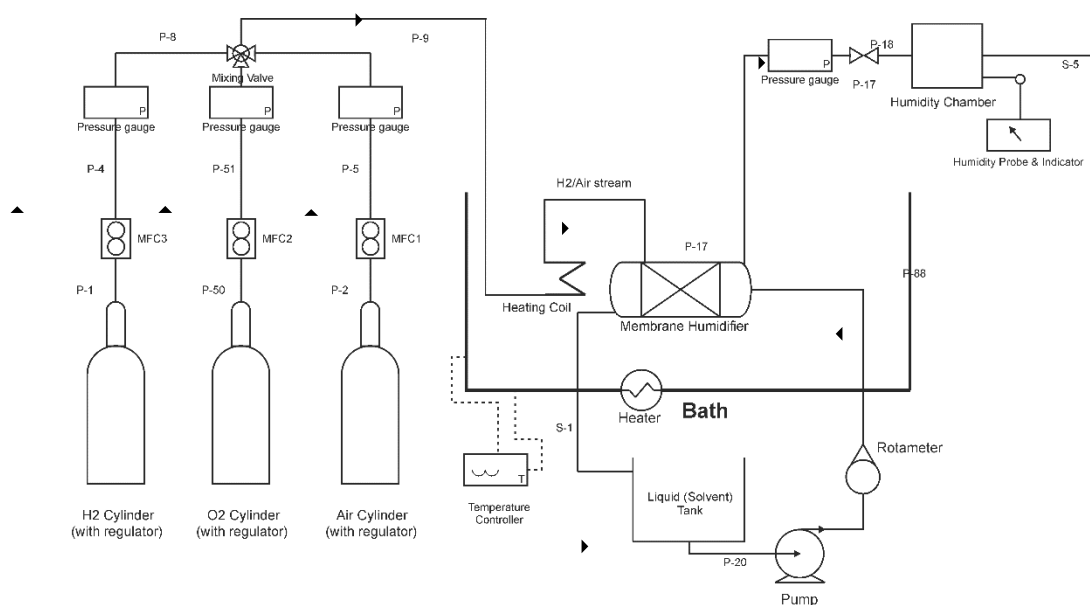| Polymer	Solvent	Polymer %	T (℃)	Tensile Strength (N/m)	Strain Break (%)	Tensile Energy Absorption (J/m²)	TENS. STIFF. (kN/m)
PSU	NMP	20.0	8.0	679.5	9.72	84.08	36.15
PSU	DMF	20.0	8.0	1.06	22.02	211.12	55.90
PSU	NMP	20.0	25.0	620.0	16.45	85.25	29.95
PSU	DMF	20.0	25.0	1.03	10.56	93.39	53.65
PSU	DMF	20.0	57.0	767.0	22.94	150.84	33.70
PSU	NMP	16.0	25.0	345.0	19.95	58.43	2.20
PSU	DMF	16.0	25.0	571.0	20.42	99.50	29.80
PSU	DMF	0.1-16.0	25.0	325.0	10.17	27.94	35.60
PSU	DMF	0.1-16.0	25.0	403.0	12.33	41.78	26.12
PES	DMF	16.0	25.0	341.33	9.04	25.80	31.70
PES	DMF	16.0	25.0	352.30	14.66	55.39	31.43
PES	NMP	16.0	25.0	312.33	11.71	29.61	33.73

Figure 1. The experimental humidification setup.

3. Neural network modeling

Artificial neural networks (ANNs) are directly inspired by the structure of the human brain, where billions of neurons are interconnected to process a variety of complex information including inputs and targets. Neural networks learn from experience and generalize from previous examples. They modify their behavior in response to the environment and are ideal in cases where the required mapping algorithm is not known or is too complex. A neural network consists of a number of simple processing elements called neurons. Each neuron in the neural network is connected to the others by means of direct links called synapse. Each synapse is associated with a parameter called weight. The neural networks are utilized to model the nonlinear relationship between inputs and outputs in an experimental process. In general, a neural network is a parallel-interconnected structure consisted of: (1) an input layer of the neuron, (2) a number of hidden layers, (3) and an output layer. A schematic view of a multilayer feed forward neural network is shown in Fig. 2. There are several types of networks and training algorithms; moreover, transfer functions can be applied for training and modeling the experimental system. The number of neurons in the input and output layers is determined by the nature of the problem. The hidden network consists of one or more layers, with several neurons in each layer. The hidden layers act like feature detectors in a black box [11,13-16].
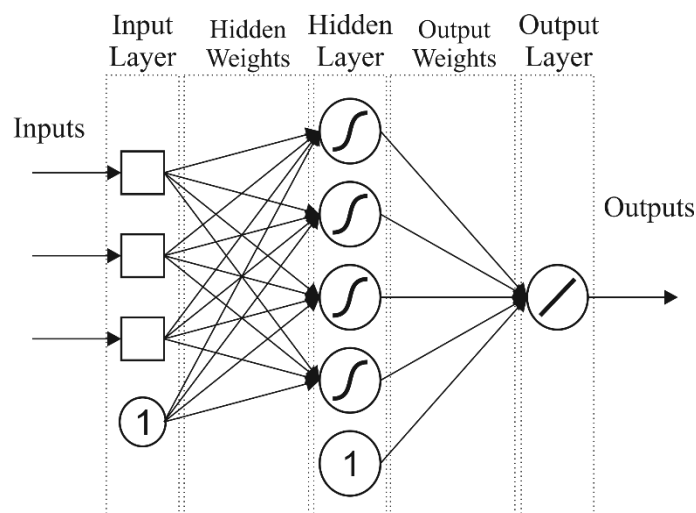
Figure 2. Schematic view of a feed forward neural network structure.

3-1. Neural network structure

The topology of an artificial neural network (ANN) is determined by the number of layers in the hidden network, the number of the neurons in each layer, and the nature of the transfer functions. Optimization of the NN topology is probably the most important step in the development of a model. In the present work, three different networks were created and trained for modeling the existing data. The first network was a Feed-Forward Back Propagation (FBP) neural network with a hidden layer including 5 neurons which were trained using *trainlm* training function. The second network was a Radial Basis Function (RBF) network, and the third one was similar to the first network except for the optimization process, which was done using Genetic Algorithm (GA).

3-2. Input data for the neural network model

Input variables for the network were as follow: (1,2) composition and material of polymeric membrane, (3) membrane thickness, (4) operating pressure, and (5) flow rate of input dry air. The output of the network was the RH percentage in the air after humidification process. The effective parameters are demonstrated in Table 3. The experimental data include the results of the mentioned 69 experiments listed in Table 1. The data were normalized and divided to two parts of 54 training data and 15 unseen test data. The training data were used for training of the neural networks and the testing data were employed for validation of the performance of the trained networks.

Table 3
Effective parameters of polymer synthesis.

Synthesis parameters				Operating parameters		
Polymer	Solvent	Polymer weight (%)	Membrane thickness (µm)	Flow rate (L/h)	Pressure (bar)	Temperature (ºC)
PSU PES	NMP DMF	7, 10, 16, 20	50, 100, 200	60, 120, 180, 300	1, 2, 3	25, 70

4. Results and discussion

In the first step, the set of input data that were unseen to the network were entered to the trained networks and the predicted outputs of RHs were obtained and reported. The results are compared in Figs. 3-6. The comparison criterion was the Relative Mean Square Error (RMSE).

$$RMSE = \sqrt{\frac{1}{N}\left(\frac{RH_{net}-RH_{exp}}{RH_{exp}}\right)^2} \qquad (1)$$

Where N is the number of input sets of data, RH_{net} is the predicted output, and RH_{exp} is the corresponding actual output.

4-1. FBP network trained using trainlm algorithm

This was a feed forward network with two layers. Five input neurons were connected to the first layer that was the hidden layer with 5 neurons inside; the next layer was output layer with one neuron which was used to calculate the output RH of the module. The network was trained using Levenberg-Marquardt (*trainlm*) back propagation algorithm. After training the network using the experimental data, corresponding outputs of 15 unseen inputs were predicted by the network. Results are shown in Fig. 3. As illustrated in Fig. 3, in comparison with the experimental data, most of the predicted outputs had little tolerance.
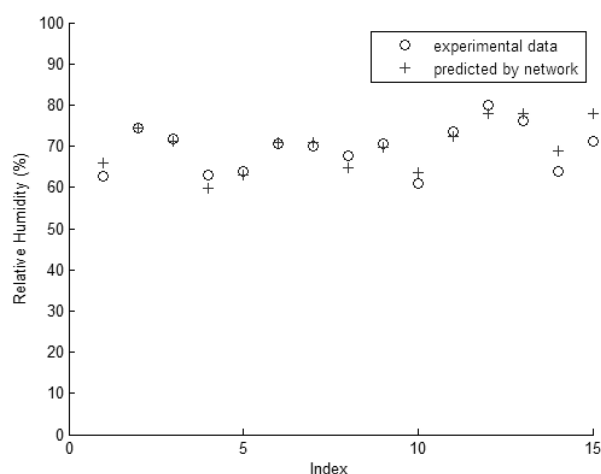

Figure 3. Test of unseen data by FBP network.

4-2. RBF network

The RBF network was trained using the experimental data and the output data were compared with the actual values as well. The RBF network had two layers. The first layer had 100 radial basis neurons. The second layer had one neuron with *purelin* transfer function. The predicted and experimental RHs are shown in Fig. 4. As shown, compared with the first network, outputs were not fitted well.
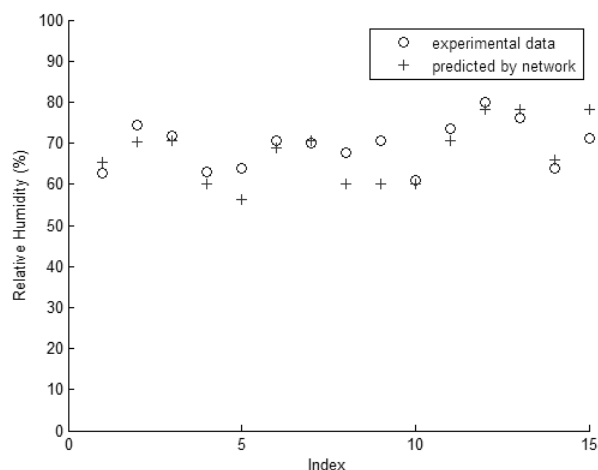
Figure 4. Test of unseen data by the RBF network.

4-3. FF network trained by GA

This was a feed forward network just like the first one, except for the training algorithm, which was not *trainlm*. Weights and biases of this network were adapted using the genetic algorithm. The predicted outputs corresponding to the unseen inputs in addition to the actual outputs of the module are illustrated in Fig. 5.
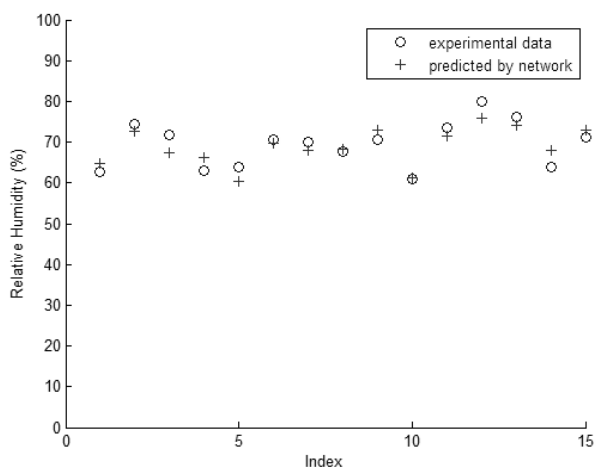

Figure 5. Test of unseen data by the FF network trained by the GA.

The RMSEs for the three networks, with different structures and training algorithms, are shown in Fig. 6. As shown, overall the RMSE of the FFGA was less than the two other networks. While some of the results of the first network were similar to those of the experimental data, however, the total error for the third network was lower than the FBP. Therefore, compared with the first and the second networks mentioned before, training of the feed forward neural network utilizing the GA was more effective and the results were better.

As shown in Fig. 6, the RMSE of the RBF was significantly more than that of the FBP and the FFGA. Although the number of neurons in RBF network was more than that in the two other networks (100 neurons in

comparison with 5 neurons), its total error was high. Thus, the radial basis transfer

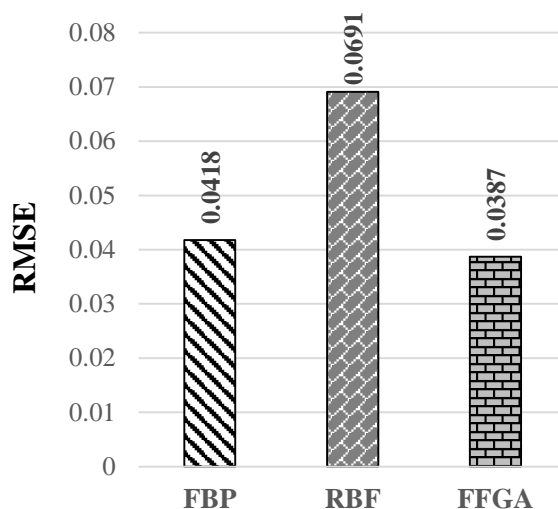function was not suitable for membrane humidifier modeling.

Figure 6. Performance of the neural networks.

5. Conclusions

The three different neural networks (FBP, RBF, and FFGA) were applied to predict the behavior of the polymer membrane humidifier using the porous membranes. The RMSE was 0.0418 for the FBP network which had 5 neurons with *tansig* transfer function in the hidden layer and it was trained by the Levenberg-Marquardt back propagation algorithm. The error of the RBF network with 100 radial basis neurons was 0.0691. The FFGA network had a structure just like the structure of the FBP. It was trained by genetic algorithm instead of back propagation. The RMSE of this network was 0.0387. Among the networks, the FFGA network showed better results. Therefore, the FFGA neural network model is a promising procedure to be used in future for modeling membrane humidifiers. The FFGA network showed better results, and had less number of neurons compared with the RBF; in addition, it had a lower RMSE than the FBP. On the other hand, the required time for training the

network with genetic algorithm was considerably more than the others. Therefore, for feasibility study, experimental data can be modeled using the FBP and the final network can be trained by the FFGA, because of its lower total error.

Abbreviations

ANN	Artificial Neural Networks
DMF	Dimethylformamide
FBP	Feed-Forward Back-Propagation
FF	Feed-Forward
FFGA	Feed-Forward Genetic Algorithm
GA	Genetic Algorithm
MLP	Multilayer Perceptron
NN	Neural Networks
NMP	N-methyl-2-pyrrolidone
PEMFC	Polymer Electrolyte Membrane Fuel Cells
RBF	Radial Basis Function
RH	Relative Humidity
RMSE	Relative Mean Square Error

References

[1] Mulder, M., *Basic principles of membrane technology*. 1996: Springer Science & Business Media.

[2] Esato, K. and Eiseman, B., "Experimental evaluation of Gore-Tex membrane oxygenator"*, J. Thorac. Cardiovasc. Surg.*, **69** (5), 690 (1975).

[3] Qi, Z. and Cussler, E., "Microporous hollow fibers for gas absorption: I. Mass transfer in the liquid"*, J. Membrane Sci.*, **23** (3), 321 (1985).

[4] Zhang, H. Y. Wang, R. Liang, D. T. and Tay, J. H., "Theoretical and experimental studies of membrane wetting in the membrane gas–liquid contacting process for CO 2 absorption"*, J. Membrane Sci.*, **308** (1), 162 (2008).

[5] Büchi, F. N. and Srinivasan, S., "Operating proton exchange membrane fuel cells without external humidification of the reactant gases fundamental aspects"*, J. Electrochem. Soc.*, **144** (8), 2767 (1997).

[6] Chen, D. Li, W. and Peng, H., "An experimental study and model validation of a membrane humidifier for PEM fuel cell humidification control"*, J. Power Sources*, **180** (1), 461 (2008).

[7] Park, S. and Oh, I. H., "An analytical model of Nafion™ membrane humidifier for proton exchange membrane fuel cells"*, J. Power Sources*, **188** (2), 498 (2009).

[8] Park, S. K. Choe, S. Y, and Choi, S. h., "Dynamic modeling and analysis of a shell-and-tube type gas-to-gas membrane humidifier for PEM fuel cell applications"*, Int. J. Hydrogen Energy*, **33** (9), 2273 (2008).

[9] Kadylak, D. and Mérida, W., "Experimental verification of a membrane humidifier model based on the effectiveness method"*, J. Power Sources*, **195** (10), 3166 (2010).

[10] Chakraborty, M. Bhattacharya, C. and Dutta, S., "Studies on the applicability of artificial neural network (ANN) in emulsion liquid membranes"*, J. Membrane Sci.*, **220** (1), 155 (2003).

[11] Fu, R. Q. Xu, T. W. and Pan, Z. X., "Modelling of the adsorption of bovine serum albumin on porous polyethylene membrane by back-propagation artificial neural network"*, J. Membr. Sci.*, **251** (1), 137 (2005).

[12] Sahoo, G. B. and Ray, C., "Predicting flux decline in crossflow membranes using artificial neural networks and genetic algorithms"*, J. Membr. Sci.*, **283** (1), 147 (2006).

[13] Shahsavand, A. and Chenar, M. P., "Neural networks modeling of hollow fiber membrane processes"*, J. Membr. Sci.*, **297** (1), 59 (2007).

[14] Al-Abri, M. and Hilal, N., "Artificial neural network simulation of combined humic substance coagulation and membrane filtration"*, Chem. Eng. J.*, **141** (1), 27 (2008).

[15] Shokrian, M. Sadrzadeh, M., and Mohammadi, T., "C_3H_8 separation from CH 4 and H 2 using a synthesized PDMS membrane: experimental and neural network modeling"*, J. Membr. Sci.*, **346** (1), 59 (2010).

[16] Liu, Y. He, G. Tan, M. Nie, F. and Li, B., "Artificial neural network model for turbulence promoter-assisted crossflow microfiltration of particulate suspensions"*, Desalination*, **338**, 57 (2014).

[17] Samimi, A. Mousavi, S. A., Moallemzadeh, A. Roostaazad, R. Hesampour, M. Pihlajamäki, A. and Mänttäri, M., "Preparation and characterization of PES and PSU membrane humidifiers"*, J. Membr. Sci.*, **383** (1), 197 (2011).